Embroidered passive UHF RFID tag on flexible 3D printed substrate

Published in
2017 Progress in Electromagnetics Research Symposium - Fall (PIERS - FALL)

DOI
10.1109/PIERS-FALL.2017.8293247

Comparison of E-textile Dipole and Folded Dipole Antennas for Wearable Passive UHF RFID Tags

Xiaochen Chen, Leena Ukkonen, Toni Björninen, and Johanna Virkki
BioMediTech Institute, Faculty of Biomedical Sciences and Engineering
Tampere University of Technology, Tampere, Finland

Abstract— We present two wearable passive UHF RFID tags based on electro-textile folded dipole and slot antennas, which have the same footprint area. We simulated the antennas in a box model and optimized them to operate near the human body. The antennas were manufactured from commercial electro-textile material by a laser cutter and reference antennas were cut from copper tape. Based on the measurement results, the attainable read ranges of the copper and electro-textile dipole tags were nearly equal and reached 2 meters. The peak read ranges of the copper and electro-textile folded dipole tags reached 2.5 meters and 2.2 meters, respectively. The results show that both simple uniplanar antennas are suitable for body area applications, but we also found the folded dipole to permit better impedance matching in this application.

1. INTRODUCTION

The development of WBAN (wireless body area network) technologies has gained a lot of research attention during the recent years, as they can offer remarkable benefits for the healthcare and welfare sectors [1–5], as well as enable novel sports-related applications [5, 6]. Passive UHF (ultra-high frequency) RFID (radio frequency identification) inspired technology has been recognized as a compelling approach to achieve versatile energy-and cost-efficient wireless technologies for future WBANs [1–4]. With the help of wearable UHF RFID equipment, the remote monitoring of movement and physiological parameters of a person can be achieved unobtrusively. The technology could be utilized in hospitals, for example in RFID-based automatic patient identification systems, and in the matching of a patient to an intended treatment. The technology can also be used for wearable wireless sensing, for example in passive moisture and strain sensors, which also have versatile possibilities in healthcare and well-being contexts [4, 7–11].

Electro-textile antennas have high potential in wearable RFID applications, as they are cost-effective, lightweight, and easy to integrate with clothes [12]. The main challenge of antenna development in body-centric systems comes from the proximity of the human body: the dielectric biological matter exhibits a notable electrical conductivity and polarizability. This leads to reduction in the antennas' radiation performance through the consumption of energy in the interaction between the antenna's electromagnetic fields and the human body. In this study, we modeled, implemented, and compared a dipole with an embedded inductive loop matching and a folded dipole having the same footprint area for wearable passive UHF RFID tags.

2. FABRICATION OF THE TAGS

Figure 1 shows the geometries and dimensions of the studied antennas, which both have a footprint area of $A = 2400\,\mathrm{mm}^2$. The electro-textile antennas were implemented by nickel and copper plated Less EMF Shieldit Super Fabric (Cat. #A1220) as the electro-textile conductor and 2 mm thick EPDM (Ethylene-Propylene-Diene-Monomer) cell rubber foam as the substrate. The electro-textile exhibits sheet resistance of approximately $0.16\,\Omega/\Box$ and the dielectric constant and loss tangent of EPDM are 1.26 and 0.007, respectively, at 915 MHz. The electro-textile material has hot melt glue on the backside and can be easily ironed on textile substrates. The electro-textile material is light-weight and conformal with the touch and feel of regular clothing. The performance of the electro-textile tags was compared with tags based on identical antennas patterned from copper tape.

The electro-textile antennas were cut by a laser cutter (Epilog Fusion Laser Model 13000). The electro-textile material can be accurately and quickly cut with a low laser power. In this case, 30% of the maximum power of 75 W was used. Laser cutting of the copper tape, on the other hand,is not feasible with a low output power. Thus, as a more appropriate tool for this material, we used

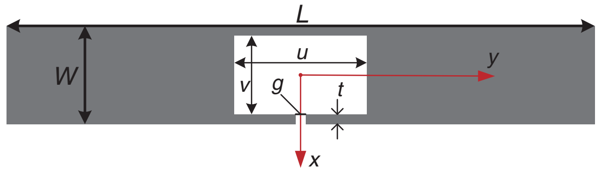

DIPOLE WITH INDUCTIVE LOOP MATCHING

t	g	L	W	u	v
2 mm	2 mm	120 mm	20 mm	27 mm	16 mm

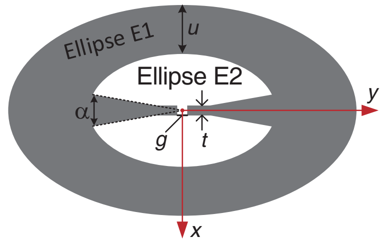

FOLDED DIPOLE

t	g	α	u	q
2 mm	2 mm	20°	10 mm	1.65

Ellipse	Semi-minor axis	Semi-major axis
E1	$\sqrt{A/(q\pi)}$	$\sqrt{(q\,.\,A)/\pi}$
E2	$\sqrt{A/q\pi} - u$	$\sqrt{(q\,.\,A)/\pi} - qu$

Figure 1: Structural diagrams of the antennas.

a vinyl cutter (Summa D60R), where an automated blade to cuts the outlines of the antennas on the copper tape.

The RFID IC (integrated circuit) used in this study was NXP UCODE G2iL RFID IC, provided in a fixture made of copper on a plastic film with $3 \times 3\,\mathrm{mm}^2$ pads. We attached the pads to the antennas using conductive epoxy (Circuit Works CW2400). The chip has a wake-up power of $-18\,\mathrm{dBm}$ ($15.8\,\mu\mathrm{W}$) and based on a previous work [13] we modelled it as a parallel connection of the resistance and capacitance of $2.85\,\mathrm{k}\Omega$ and $0.91\,\mathrm{pF}$, respectively. Fig. 2 shows the ready-made tags.

Figure 2: (a) Ready-made copper dipole and (b) electro-textile folded dipole RFID tags.

3. SIMULATIONS AND WIRELESS MEASUREMENTS

To account for the influence of the human body on the electromagnetic properties of the antennas, we simulated themaffixed on a $26\,\mathrm{cm} \times 50\,\mathrm{cm} \times 59.5\,\mathrm{cm}$ rectangular block of dielectric material having the dielectric properties of the human skin (the relative permittivity is 76.11 and the conductivity is $0.48\,\mathrm{S/m}$ at $915\,\mathrm{MHz}$). Fig. 3 presents the antenna structure and simulation model and indicates the tag placement in the skin block model. It corresponds to the center of the upper back in between the scapula. The software package we used in antenna modeling and optimization was ANSYS HFSS with the target of maximal tag read range at $915\,\mathrm{MHz}$.

Normally, the read range of the passive tags is limited by the forward link operation. In free space, the attainable read range of the tag at the spatial observation angles φ and θ of a spherical

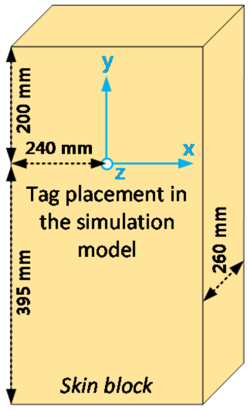

Figure 3: The simplified model of the human torso used in the antenna modelling. The coordinate axes correspond with Fig. 1.

coordinate system centered at the tag is given by:

$$d_{tag}\left(\varphi,\theta\right) = \frac{\lambda}{4\pi}\sqrt{\frac{\tau e_r D\left(\varphi,\theta\right) EIRP}{P_{ic0}}}, \tag{1}$$

$$\tau = \frac{4\mathrm{Re}\left(Z_A\right)\mathrm{Re}\left(Z_{IC}\right)}{\left|Z_A+Z_{IC}\right|^2}, \tag{2}$$

where λ is the wavelength of the reader' continuous-wave signal energizing the tag, $EIRP$ is the regulated equivalent isotropic radiated power, P_{ic0} is the wake-up power of the tag IC, e_r is the tag antenna radiation efficiency, D is the directivity of the tag antenna, τ is the antenna-IC power transfer efficiency determined by the impedances of the antenna (Z_A) and IC (Z_{IC}).

To estimate d_{tag} of the manufactured tags, we tested them wirelessly with Voyantic Tagformance system. It is based on an RFID reader with an adjustable transmission frequency (0.8 . . . 1 GHz) and output power (up to 30 dBm) and provides the recording of the backscattered signal strength (down to −80 dBm) from the tag under test. Estimation of d_{tag} was done by characterizing the wireless channel from the reader antenna to the location of the tag under test and by recording the smallest output power of the reader (threshold power) at which a valid 16-bit random number from the tag is received as a response to the query command in ISO 18000-6C communication standard. First, the power loss factor (L_{iso}) between the reader and the tag was obtained as $L_{iso} = \Lambda/P_{th^*}$, where Λ is a constant provided by the system manufacturer to describe the sensitivity of the reference tag at each frequency, P_{th*} is the measured threshold power of the reference tag. The incident threshold power density at the tag's location is given by:

$$S_{inc,th} = \frac{L_{iso}P_{th}}{\lambda^2/4\pi} = \frac{4\pi\Lambda}{\lambda^2 P_{th*}}P_{th}, \tag{3}$$

where λ is the wavelength and P_{th} is the measured threshold power of the tag under test. Thus, d_{tag} can be expressed as

$$d_{tag}\left(P_{th},P_{th*}\right) = \sqrt{\frac{EIRP}{4\pi S_{inc,th}}} = \frac{\lambda}{4\pi}\sqrt{\frac{EIRP}{\Lambda}\frac{P_{th*}}{P_{th}}}, \tag{4}$$

where $EIRP = 3.28\,\mathrm{W}$, according to RFID emission limits in Europe.

In the wireless measurements, we attached each tag in the upper back of a standing male test subject. The tags were attached so that the substrate under the tag was affixed directly on skin and were worn underneath regular cotton shirt during the measurements. The measurements were conducted in an anechoic chamber at the distance of one meter.

4. RESULTS AND DISCUSSION

The simulated impedance of the antenna in the box model is shown in Fig. 4. The reactances of the antennas are practicallythe same with different materials, but the electro-textile antennas exhibit slightly higher resistance compared with the copper ones. This correlates with the lower conductivity of the electro-textile material. As can be seen from Fig. 5, the main difference between the dipole and folded dipole antennas is that the folded dipole antenna achieves better impedance matching. According to our parametric studies, it was not possible to achieve better impedance matching for the dipole antenna in the body-worn configuration by using the embedded inductive loop matching, due to the inherently elevated antenna resistance. However, as shown by the further results discussed below, the radiation properties of the dipole were better than those of the folded dipole.

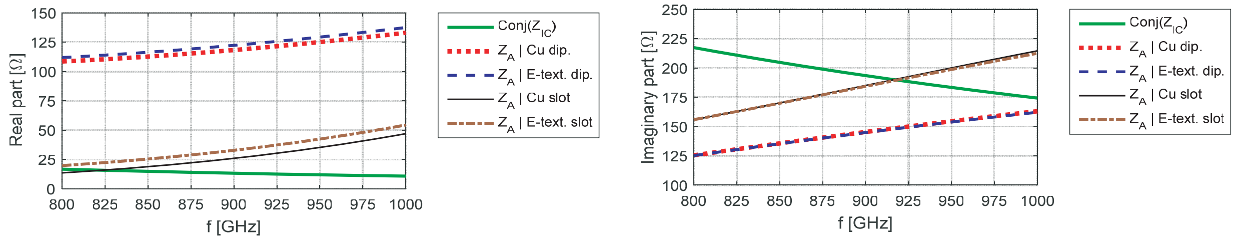

Figure 4: Simulated antenna impedance in the box model and the conjugate of the microchip impedance from the parallel RC equivalent circuit model ($R = 2.85\,\mathrm{k}\Omega$, $C = 0.91\,\mathrm{pF}$).

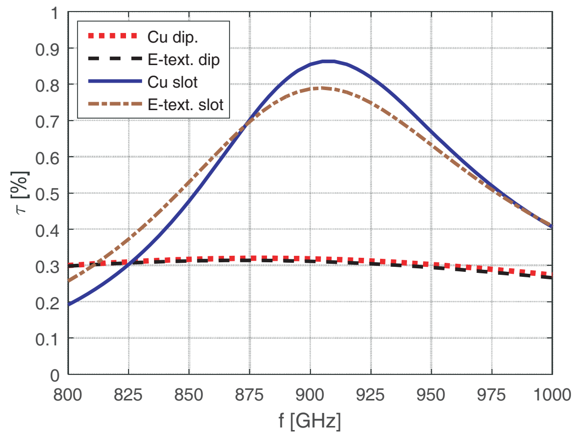

Figure 5: Simulated antenna-microchip power transfer efficiency.

Table 1 compares the directivity, radiation efficiency, gain, and power transfer efficiency of each tag in the at different global UHF frequencies. In the table, the conductor material did not affect the radiation properties noticeably. The directivities of the dipole and folded dipole were also similar. However, the dipole antenna provided a much higher radiation efficiency and thereby higher gain. Conversely, we found the antenna-IC power transfer efficiency attainable with the embedded loop matching approach applied in the dipole limited, whereas we achieved a good complex conjugate impedance matching using the folded dipole.

Figure 6 presents the simulated and measured d_{tag} of all the studied tags. For the copper and electro-textile dipole tags, the measured read rangeswere around 2 meters. In addition, the frequency trend of the read range was nearly flat in the whole frequency band, which corresponds with the same trend predicted for τ in Fig. 5. For the folded dipole tag, d_{tag} peaked at around 2.5 meters and 2 meters for the copper tape and electro-textile version, respectively. Overall, the simulations predicted the level and frequency trend of the measured d_{tag} extremely well for all studied tags. Notably, the performance of the electro-textile tags was highly comparable to the tags with copper antennas. This is promising for wearable applications where the tags must be seamlessly integrated with regular clothing. It should be noted, however, that the performance of the tag could significantly change when attached to other parts of the human body, as has been previously studied in the case of a slotted patch antenna [14], for instance.

Table 1: Summary of the antenna radiation properties.

	Freq. [MHz]	Cu dip.	E-text. dip.	Cu folded dip.	E-text. Folded dip.
D [dBi]	860	6.26	6.26	6.01	6.01
	915	6.47	6.49	6.21	6.21
	960	6.56	6.56	6.21	6.21
e_r [%]	860	1.81	1.70	1.09	0.78
	915	1.90	1.79	1.19	0.94
	960	2.00	1.88	1.32	1.09
G [dBi]	860	−11.2	−11.4	−13.8	−15.1
	915	−10.7	−11.0	−13.0	−14.1
	960	−10.4	−10.7	−12.6	−13.4
τ [%]	860	32	31	57	61
	915	32	31	86	78
	960	30	29	60	56

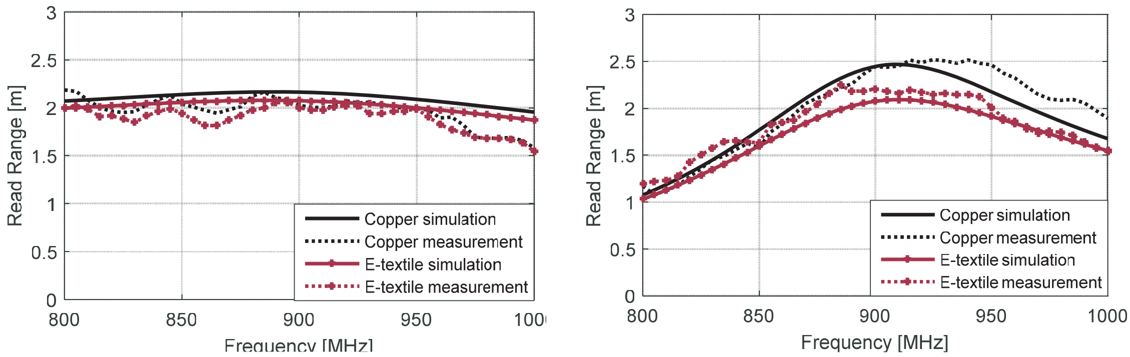

Figure 6: Measured and simulated attainable read range of the (a) dipole and (b) folded dipole tags in the direction of the positive z-axis shown in Fig. 3.

5. CONCLUSIONS

We presented a comparison of wearable passive UHF RFID tags based on a dipole with embedded inductive loop matching and a folded dipole having equal footprint sizes. Antennas for both tag types were modelled and optimized using a simplified model where a homogenous dielectric block represented the human torso. The antennas were fabricated from copper tape and electro-textile material and the performance of each tag attached to the upper back of a test subject was assessed through wireless measurement. Our results showed that both of the studied uniplanar antennas are fit for wearable tags and provide similar performance in terms of the tag read range, but we also found the folded dipole to permit better impedance matching in this application.

REFERENCES

1. Sani, A.. M, Rajab, R. Forster, and Y. Hao, "Antennas and propagation of implanted RFIDs for pervasive healthcare applications," *Proc. IEEE*, Vol. 98, No. 9, 1648–1655, Sep. 2010.
2. Marrocco, G., "RFID antennas for the UHF remote monitoring of human subjects," *IEEE Trans. Antennas Propag.*, Vol. 55, No. 6, 1862–1870, Jun. 2007.
3. Grosinger, J., "Feasibility of backscatter RFID system on the human body," *EURASIP J. Embedded Syst.*, Vol. 2013, No. 2, 10, Mar. 2013.
4. Merilampi, S., H. He, L. Sydänheimo, L. Ukkonen, and J. Virkki, "The possibilities of passive UHF RFID textile tags as comfortable wearable sweat rate sensors," *2016 Progress in Electromagnetic Research Symposium (PIERS)*, 3984–3987, Shanghai, China, Aug. 8–11, 2016.
5. Tsolis, A., W. G. Whittow, A. Alexandridis, and J. Vardaxoglou, "Embroidery and related manufacturing techniques for wearable antennas: Challenges and opportunities," *Electronics*, Vol. 3, No. 2, 314–338, May 2014.

6. Salvo, P., F. Di Francesco, D. Costanzo, C. Ferrari, M. G. Trivella, and D. De Rossi, "A wearable sensor for measuring sweat rate," *IEEE Sensors J.*, Vol. 10, No. 10, 1557–1558, Oct. 2010.
7. Liu, Y., A. Levitt, C. Kara, C. Sahin, G. Dion, and K. R. Dandekar, "An improved design of wearable strain sensor based on knitted RFID technology," *Proc. IEEE CAMA*, 4, Syracuse, NY, USA, 2016.
8. Shinmoto Torres, R. L., D. C. Ranasinghe, Q. Shi, and A. P. Sample, "Sensor enabled wearable RFID technology for mitigating the risk of falls near beds," *Proc. IEEE RFID Intl. Conf.*, 191–198, Orlando, FL, USA, 2013.
9. Kaufmann, T., D. C. Ranasinghe, M. Zhou, and C. Fumeaux, "Wearable quarter-wave folded microstrip antenna for passive UHF RFID applications," *Intl. J. Antennas Propag.*, Vol. 2013, Article ID 129839, 11, May 2013.
10. Rakibet, O. O., C. V. Rumens, J. C. Batchelor, and S. J. Holder, "Epidermal passive RFID strain sensor for assisted technologies," *IEEE Antennas Wireless Propag. Lett.*, Vol. 13, 814–817, Apr. 2014.
11. Amendola, S., G. Bovesecchi, P. Coppa, and G. Marrocco, "Thermal characterization of epidermal RFID sensor for skin temperature measurements," *Proc. IEEE AP-S Intl. Symp. Antennas Propag.*, 461–462, Puerto Rico, USA, 2016.
12. Fu, Y. Y., Y. L. Chan, M. H. Yang, Y.-C. Chan, J. Virkki, T. Björninen, L. Sydänheimo, and L. Ukkonen, "Experimental study on the washing durability of electro-textile UHF RFID tags," *IEEE Antennas Wireless Propag. Lett.*, Vol. 14, 466–469, 2015.
13. Björninen, T., L. Sydänheimo, and L. Ukkonen, "Development and validation of an equivalent circuit model for UHF RFID IC based on wireless tag measurements," *Proc. AMTA Symp.*, 6, Bellevue, WA, USA, 2012.
14. Virkki, J., Z. Wei, A. Liu, L. Ukkonen, and T. Björninen, "Wearable passive e-textile UHF RFID tag based on a slotted patch antenna with sewn ground and microchip interconnections," *Intl. J. Antennas Propag.*, Vol. 2017, Article ID 3476017, 8, Feb. 2017.